Journal of Peptide Science
J. Pept. Sci. 2008; **14**: 528–534
Published online 21 December 2007 in Wiley InterScience (www.interscience.wiley.com). DOI: 10.1002/psc.993

JOURNAL OF PEPTIDE SCIENCE

Membrane structure and interactions of a short Lycotoxin I analogue‡

R. ADÃO,[a] R. SEIXAS,[a] P. GOMES,[a] J. COSTA PESSOA[b] and M. BASTOS[a]*

[a] CIQ (UP), Department of Chemistry, Faculty of Sciences, University of Porto, P-4169-007 Porto, Portugal
[b] Centro de Química Estrutural, Instituto Superior Técnico, TU Lisboa, P-1049-001, Lisboa, Portugal

Received 5 July 2007; *Revised 23 October 2007*; *Accepted 2 November 2007*

Abstract: Lycotoxin I and Lycotoxin II are natural anti-microbial peptides that were identified in the venom of the Wolf Spider *Lycosa carolinensis*. These peptides were found to be potent growth inhibitors for bacteria (*Escherichia coli*) and yeast (*Candida glabrata*) at micromolar concentrations. Recently, shortened analogues of LycoI and LycoII have been reported to have decreased haemolytic effects. A shorter Lyco-I analogue studied, LycoI 1–15 (H-IWLTALKFLGKHAAK-NH_2), was active only above 10 μM, but was also the least haemolytic.

On the basis of these findings, we became interested in obtaining a deeper insight into the membrane activity of LycoI 1–15, as this peptide may represent the first major step for the future development of selective, i.e. non-haemolytic, Lycotoxin-based antibiotics.

The interaction of this peptide with liposomes of different composition was studied by microcalorimetry [differential scanning calorimetry (DSC) and isothermal titration calorimetry (ITC)] and CD. The results obtained from the calorimetric and spectroscopic techniques were jointly discussed in an attempt to further understand the interaction of this peptide with model membranes.

Keywords: microcalorimetry; ITC; DSC; anti-microbial peptide; model membranes

INTRODUCTION

Anti-microbial peptides have been widely studied in the past years [1–15], as they may become an alternative to conventional antibiotic therapy, in view of the growing emergence of multi-resistant microbial strains. Substantial efforts have been directed to increase the potency and specificity of these peptides against pathogenic agents, while minimizing their deleterious effects towards eukaryotic cells. Although the detailed mode of action of anti-microbial peptides is not well established and, further, it is now known that it differs for distinct peptides, it is clear that all cationic amphipathic peptides interact with membranes. It has been proposed that the cytoplasmic membrane is the main target for some of these peptides, and therefore, the development of resistance is not to be expected [8].

Lycotoxin I (LycoI, H–IWLTALKFLGKHAAKHLAKQQL SKL–NH_2) and Lycotoxin II (LycoII, H–KIKWFKTMKSIA KFIAKEQMKKHLGGE–OH) are natural anti-microbial peptides that were identified in the venom of the Wolf Spider *Lycosa carolinensis* [16]. They were found to be potent growth inhibitors for bacteria (*Escherichia coli*) and yeast (*Candida glabrata*) at micromolar concentrations. Their secondary structure was predicted to be an amphipathic α-helix, a structure that is common in pore-forming peptides [16]. Recently, these peptides were found to be active against *Leishmania donovani* promastigotes and *Leishmania pifanoi* amastigotes, also at the micromolar range, with LycoI being the most active peptide [17]. The serious drawback of these natural peptides (especially LycoI) is their significant haemolytic activity above 20 μM, studied against rabbit and sheep erythrocytes [16,17], which severely limits their potential application as antibiotics.

The specificity of a drug for bacteria over erythrocytes, or its therapeutic index, defined as the ratio of minimal haemolytic concentration (MHC) to minimal inhibitory concentration (MIC), can be increased as follows: (i) by only increasing its anti-microbial activity, (ii) by decreasing haemolytic activity while maintaining anti-microbial activity, or (iii) ideally, by combining an increase in anti-microbial activity with a decrease in haemolytic activity.

Recently, shortened analogues of LycoI and LycoII have been reported in a study where *C*-terminal shortening of LycoI is shown to lower the peptide's leishmanicidal activity, but with the advantage of showing decreased haemolytic effects. Thus, the shorter LycoI analogue studied, LycoI 1–15 (H–IWLTALKFLGKHAAK–NH_2) was only active above 10 μM, but was also the least haemolytic of the set [17]. So, although not all goals described above in terms of increased therapeutic index were achieved, we

*Correspondence to: M. Bastos, CIQ (UP), Department of Chemistry, Faculty of Sciences, University of Porto, P-4169-007 Porto, Portugal; e-mail: mbastos@fc.up.pt
‡ This article is part of the Special Issue of the Journal of Peptide Science entitled "2nd workshop on biophysics of membrane-active peptides".

became interested in obtaining a deeper insight into the membrane activity of LycoI 1–15, as this peptide may represent the first major step for the future development of selective, i.e. non-haemolytic, Lycotoxin-based antibiotics.

Differential scanning calorimetry (DSC) has emerged as a most valuable tool to study peptide–membrane interactions [1,15,18–23]. DSC analysis provides a thermodynamic characterization of the changes induced by peptides on lipid bilayer phase transitions. Membrane interfaces have the ability to induce secondary structure in a wide range of anti-microbial peptides [21,24–27]. The change in the secondary structure of the peptide upon interaction with the membranes can be evaluated by CD spectroscopy. Using isothermal titration calorimetry (ITC), we can determine the energetics of the interaction of the peptides with model membranes of different composition.

We herein report the study of the interactions between the anti-microbial peptide LycoI 1–15 (H-IWLTALKFLGKHAAK-NH_2) and large unilamellar vesicles (LUVs) of three different lipid bilayer systems: zwitterionic 1,2-dimyristoyl-*sn*-glicero-3-phosphocholine (DMPC), anionic 1,2- dimyristoyl-*sn*- glycero-3-[phospho- *rac*-(1-glycerol)] (DMPG) and a DMPC/DMPG (3 : 1) mixture. The importance of membrane composition in the interaction processes, as reflected in the differences found here, represents a contribution to the understanding of peptide-induced lipid bilayer permeabilization and the mode of action of LycoI 1–15 on biological level.

MATERIALS AND METHODS

Materials

DMPC and DMPG were obtained from Avanti Polar Lipids (Alabaster, AL, USA), and used without further purification. Fmoc-protected amino acids, coupling reagents and resins for solid-phase peptide synthesis were purchased from Bachem (Weil am Rhein, Germany). *N*-(2-hydroxyethyl) piperazine-*N*′-ethane-sulphonic acid (HEPES) was from Sigma Chemical Co. (St Louis, MO, USA). Ultra pure water (Milli Q Gradient, Millipore, Billerica, MA, USA) was used in the preparation of all samples. All other chemicals were from Sigma Chemical Co. (St Louis, MO, USA).

Preparation of Liposomes

Appropriate amounts of phospholipids (DMPC, DMPG and DMPC/DMPG (3 : 1)) were dissolved in chloroform (DMPC) or chloroform/methanol ((3 : 1) v/v) (DMPG and DMPC/DMPG (3 : 1)). The samples were then dried under a nitrogen stream, and the film was kept under vacuum for 3 h to remove all traces of organic solvents. The resulting lipid film was warmed together with HEPES buffer (10 mM; 0.1 M NaCl; pH = 7.4) in a thermostated water bath at *ca* 10 °C above the temperature of the gel-to-liquid crystalline phase transition (T_m), and then hydrated at the same temperature. The multi-lamellar vesicles (MLVs) thus obtained were frozen in liquid nitrogen and thawed in a water bath at *ca* 10 °C above T_m, and this process was repeated 5 times.

LUVs were obtained from the MLVs by extrusion in a 10 ml stainless steel extruder (Lipex Biomembranes, Vancouver, BC, Canada), inserted in a thermostated cell with a recirculating water bath, at *ca* 10 °C above T_m. The samples were passed several times through polycarbonate filters (Nucleopore, Pleasanton, CA, USA) of decreasing pore size (600, 200 and 100 nm; 5, 5 and 10 times, respectively), under inert nitrogen atmosphere.

Size distribution of extruded vesicles was determined by DLS (Zetasizer nanoZS, Malvern Instruments, Malvern, Worcestershire, UK) at 37 °C, using a He–Ne laser (wavelength 633 nm) as a source of incident light, and operating at a scattering angle of 173°. Mean particle size was thus determined as being (106 ± 4) nm (average and standard deviation of 6 independent measurements). The phospholipid concentration was determined by the phosphomolybdate method [28].

Preparation of Peptides

The peptide was synthesized as *C*-terminal carboxamides by Fmoc/^{t}Bu solid phase strategies, purified and characterized by methods as those described in Gomes *et al.* [29]. Peptide stock solutions were prepared in HEPES buffer (10 mM; 0.1M NaCl; pH = 7.4) in the 2–5 mM concentration range, and quantitated by AAA (amino acid analysis).

Differential Scanning Calorimetry

DSC was performed in a microcalorimeter (Micro-DSCIII, SETARAM, Caluire, France). The experiments with liposome suspensions or (liposome + peptides) were run against HEPES buffer in the reference cell. Blank experiments with HEPES buffer on both cells were also performed for subsequent baseline correction. The solution or suspension volume used in each cell was about 0.8 ml, and the masses of sample and reference cells were adjusted by weight to ±0.00005 g. Two successive up- and down-scans were performed for each sample, the up-scan at a scanning rate of 0.5 °C/min and the down-scan at 3 °C/min, over a temperature (t) range of 10–35 °C. The sample mixtures were prepared immediately before the DSC run, by adding the desired amount of peptide stock solution to the suspension of LUVs. Separate runs for each liposome suspension without peptide were also done. All procedures regarding sample preparation and handling (lag time at low temperature, time between mixture preparation and start of the experiment) were kept constant in all experiments to ensure that all samples had the same thermal history. The instrument was electrically calibrated for temperature and scan rate.

The Micro-DSCIII software was used for baseline subtraction, calculation of the gel-to-liquid crystalline phase transition temperature (T_m) and transition enthalpy (ΔH). T_m and ΔH were calculated by integration of the heat capacity (Cp) *versus* temperature (t) curve. For consistency and comparability, the integration was always done between the two points: one from where the curve starts to deviate and the other where it returns to the baseline.

DOI: 10.1002/psc

Isothermal Titration Calorimetry

The calorimetric technique used was stepwise isothermal titration microcalorimetry. The water bath and peripheral units were built at Lund University, and a twin heat conduction calorimeter (ThermoMetric AB, Järfälla, Sweden) was used with a 1 cm^3 titration cell equipped with a gold stirrer. The instrument was electrically calibrated using an insertion heater [30]. The detailed calorimetric set-up and basic procedure has been described previously [31]. Briefly, in each titration, 0.9848 ± 0.0008 ml of liposome suspension was placed in the titration cell and sequences of successive injections were made at 4 min intervals (injections with 20 min interval did not reveal the presence of slow reactions). The temperature of the measurements was 35 °C throughout, so that the recorded values refer to the interaction of the peptides with the liposomes in the fluid phase [1]. Experiments were performed in the 'fast titration mode', the resultant curves were deconvoluted [32] and the integrals were calculated, and transformed to heat exchanged by the appropriate calibration constant. The obtained heats were corrected for the dilution effects as determined in separate experiments.

The experimental set-up used corresponds to very low P : L ratios (about 1 : 3000), where 7.006 μl of peptide solutions (1.4 mM) were injected into the liposome suspension (35 mM) contained in the cell.

Circular Dichroism

CD measurements were carried out in a Jasco 720 spectropolarimeter, with a 175–800 nm photomultiplier (Japan Spectroscopic Co., Tokyo), using a cylindrical cell of 1 mm path length. Experimental conditions were as follows: 0.5 nm bandwidth, 50 mdeg sensitivity, 1 nm resolution, 1 s time response, discrete wavelength readings (1 nm). In most cases, each spectrum was the average of six accumulations but, when the signal-to-noise ratio was too low, a higher number (up to 24) of accumulations was used. Buffer runs were repeated throughout the day to check for repeatability. Spectra of pure liposomes at different concentrations were run as blanks to be subtracted from the liposome/peptide spectra. After blank correction, the observed ellipticity was converted to mean residue molar ellipticity (θ) (deg cm^2 $dmol^{-1}$).

The measurements in buffer were done with peptide concentrations of 36 μM, and in the mixtures the peptide was added to the lipid suspensions immediately before measurement. A concentration of 6000 μM was used for DMPC with a peptide–lipid molar ratio of 1 : 79, and a concentration of 1200 μM for DMPG and DMPC/DMPG (3 : 1) with a peptide–lipid molar ratio of 1 : 32. All spectra were recorded at 35 °C, with the temperature kept constant by a circulating water bath.

RESULTS

In Figure 1, we show a helical wheel representation of LycoI 1–15, a perfect amphipatic α-helix, with all charged residues on one face of the helix. This characteristic indicates that, probably, it will interact with different types of membranes.

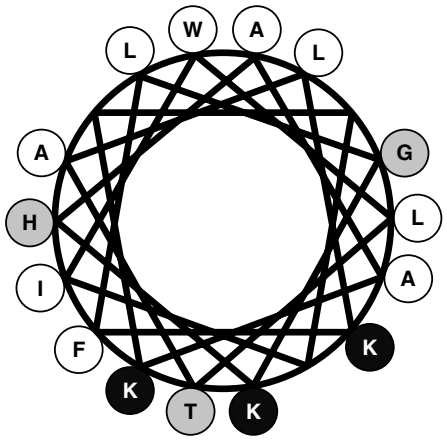

Figure 1 Helical wheel representation of Lyco I 1–15. Light grey – polar, non-charged residues; dark grey – polar, positively charged residues; white – hydrophobic residues.

In Figure 2(A)–(C) we plot the C_p *versus* t curves for the gel-to-liquid crystalline phase transition of the lipid bilayer, at increasing peptide ratios (DMPC, DMPG and DMPC/DMPG (3 : 1)), respectively. The calculated thermodynamic parameters are listed in Table 1, where values for the pure lipid systems are also shown. Measurements on the same peptide/lipid systems were always done using a liposome suspension from the same preparation batch, to avoid slight differences that might arise from different preparation, as small differences in T_m and ΔH can be observed for the same pure lipid system in different preparation batches. The estimated error between samples is larger and is also provided in the footnote of Table 1.

It can be seen that LycoI 1–15 interacts with all model systems, although to a different degree, as reflected by changes in the transition temperature, T_m and the enthalpy of the transition, ΔH. For the DMPC system (Figure 2(A)), both T_m and ΔH decrease as the peptide content in the mixture increases, whereas for the DMPG (Figure 2(B)) the temperatures remain constant and the enthalpies decrease until a molar ratio of 1 : 71. At the molar ratio of 1 : 23, the curve with DMPG is completely distorted indicating a high degree of liposome destruction. As for DMPC, we can see the onset of two transitions at 1 : 71, one at a lower temperature and a shoulder at a higher temperature. As the peptide content increases, the relative importance of the lower temperature peak also increases, its shape becomes sharper and its temperature decreases. In Table 1, we report the values of T_m for both peaks and the total ΔH, as well as the individual contributions.

In the case of the mixed membrane, although the general appearance is intermediate between the two previous systems, the profile is more close to the one observed with the negatively charged system until a molar ratio of 1 : 71, as up to this peptide–lipid molar ratio the curve is not as distorted as in the DMPC

DOI: 10.1002/psc

Table 1 Transition temperatures, T_m, and enthalpy change values, ΔH, for the gel-to-liquid crystal liposome transition as a function of peptide–lipid molar ratio (P : L) for the three lipid systems

(P : L) ratio	DMPC			DMPG			DMPC/DMPG(3 : 1)		
	T_m/°C[a]	ΔT_m/°C[b]	ΔH/kJ.mol^{-1}[c]	T_m/°C	ΔT_m/°C	ΔH/kJ.mol^{-1}	T_m/°C	ΔT_m/°C	ΔH/kJ.mol^{-1}
Pure lipid	24.7	—	22	23.8	—	26	24.9	—	23
(1 : 143)	24.3	0.4	17	23.6	0.2	23	24.6	0.3	17
(1 : 95)	—	—	—	23.4	0.4	20	24.2	0.7	18
(1 : 71)	23.4	1.3	16	23.0	0.8	21	23.7	1.2	25
(1 : 35)	21.6	3.1	12 (8 + 4)	—	—	—	—	—	—
	26.4	−1.7	—						
(1 : 23)	20.7	4	15 (8 + 7)	19.6	4.2	19 (6 + 13)	—	—	—
	24.7	0	—	24.5	−0.7	—			

[a] The estimated uncertainty in T_m is ±0.3 °C and in ΔH it is ±0.5 kJ mol^{-1} (for the same liposome suspension) and ±3 kJ mol^{-1} (for liposome suspensions from different preparations).
[b] ΔTm/°C = $T_{m\ (pure\ lipid)} - T_{m\ (lipid+peptide)}$
[c] The reported enthalpy corresponds to the total peak area and within brackets are the separate enthalpies when a significant peak splitting is observed.

system. This is to be expected as the electrostatic contribution to the interaction is very significant.

For all peptide/liposome mixtures, precipitation and aggregation were observed, which were more pronounced for the DMPG system. Further, the onset of precipitation with DMPC was much slower than with the negatively charged systems.

The ITC tracings for the titration of LycoI 1–15 into DMPC and DMPG suspensions are shown in Figure 3(A) and (B) LycoI 1–15 interacts exothermally with both systems, the interaction being strongest with DMPG. The titrations were performed at very low peptide–lipid ratios (1 : 3000). After integration of the observed peaks and correction for dilution of the peptides into buffer, the enthalpy of interaction (per mole of total injected peptide) can be calculated as -39 ± 6 and -63 ± 10 kJ mol^{-1} for DMPC and DMPG, respectively. This value will be corrected later to the peptide content in the membrane using the CD results.

Figure 4 shows the CD spectra of the peptide for the three model systems. LycoI 1–15 shows predominantly a random coil structure in HEPES buffer, and forms an α-helix in the presence of all three membrane systems. Nevertheless, the characteristic minima at 208 and 222 nm of an α-helix shows the most negative θ values for DMPG, followed closely by DMPC/DMPG. The CD spectra for the interaction of LycoI 1–15 with DMPC shows almost the same position of the minima but with much smaller θ values, even though we increased the liposome concentration to 6000 μM (whereas it was 1200 μM for the other systems). This reflects a lower partition to the zwitterionic membrane, although keeping the same secondary structure, as the CD signal in peptide–liposome systems is a weighed mixture of the various forms present in solution. Moreover, in order to get clear results with the zwitterionic system, we had to incubate the mixture for 1/2 h at 35 °C prior to measurement, showing that the partition to the zwitterionic membrane is a slow process, in contrast to partition to negatively (or partly negatively) charged systems. We already found the same behaviour in a previous study involving two anti-microbial peptides that were hybrids from Cecropin A and Melittin [1]. Considering that the partition to DMPG is 100% (complete binding) and that the peptide binds to all systems with the same structure, we can estimate from the respective θ values at 222 nm that we will have bound fraction values of ~89 and ~38% for the DMPC/DMPG and DMPC systems, respectively. The assumption of close to 100% partition to the purely negatively charged membrane will, indeed, provide an upper bound to the results, but it is reasonable for our purpose. From these bound fractions and the known total amount of peptide present in each case, partition constants of about 10^4 and 1.5×10^2 can be derived for DMPC/DMPG and DMPC systems, respectively. Finally, from these values we can estimate an upper bound to the amount of peptide that partitions to DMPC, and use it to correct the enthalpy value that was obtained by ITC. The resulting corrected value is −50 kJ mol^{-1}.

DISCUSSION

The biological activity of anti-microbial peptides has been largely associated to their interaction with membranes. This interaction indeed depends on both the peptide and the membrane composition.

The results described above for the interactions of LycoI 1–15 with three lipid bilayer systems allow us to shed some light onto the peptide–membrane

DOI: 10.1002/psc

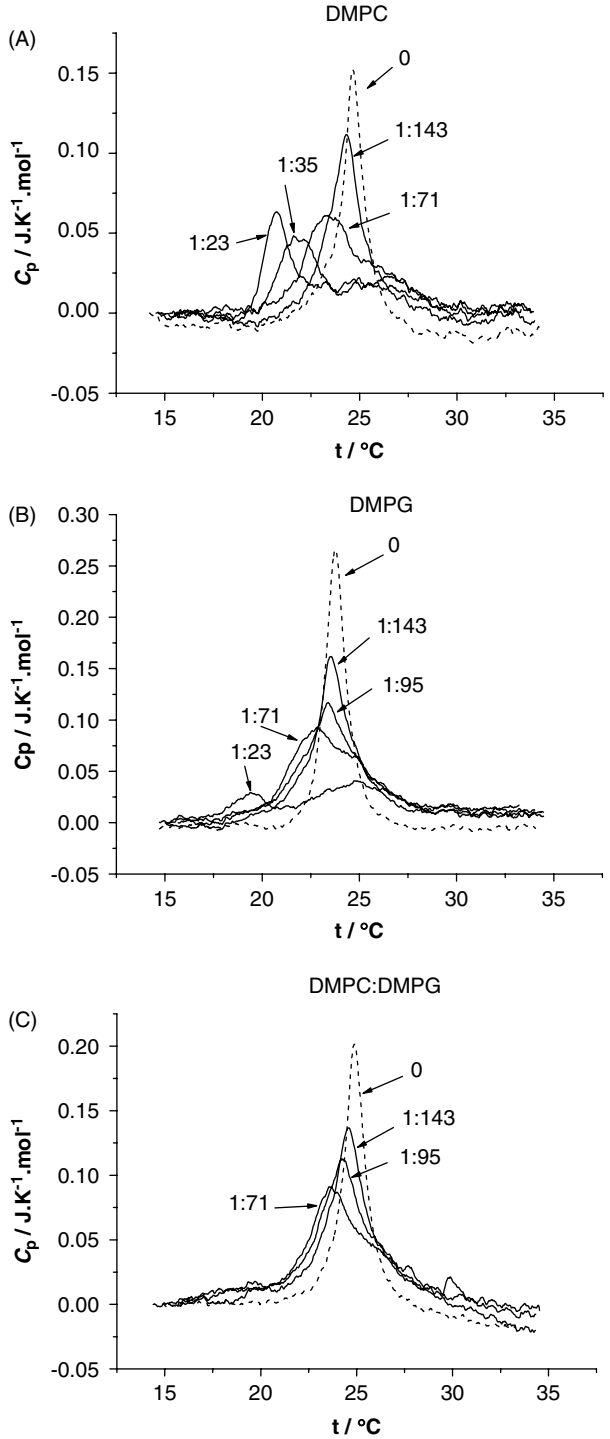

Figure 2 DSC curves obtained for liposomes and Lyco I (1–15) for pure liposomes and different peptide–lipid molar ratios (P : L): DMPC (A), DMPG (B), DMPC/DMPG (3 : 1) (C). The peptide molar ratio for each profile is indicated in the figure. Lipid concentration was 3.0 ± 0.3 mM in all experiments.

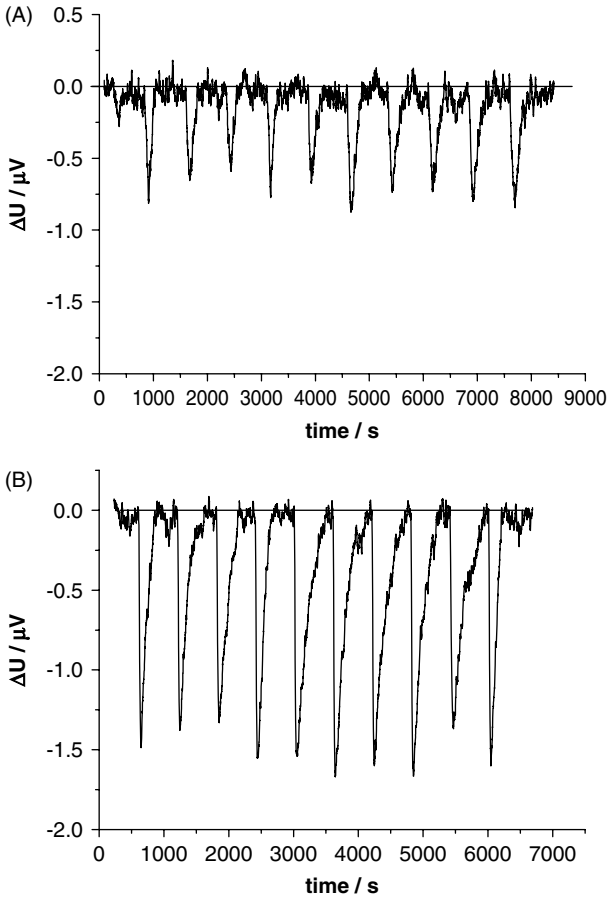

Figure 3 **(A)** Raw data (potential difference across the thermopiles as a function of time) for the titration of Lyco I 1–15 ($c = 1.4$ mM) into DMPC suspension in the vessel ($c = 35$ mM). The volume per injection was 7.006 μl. **(B)** Raw data (potential difference across the thermopiles as a function of time) for the titration of Lyco I 1–15 ($c = 1.5$ mM) into DMPG suspension in the vessel ($c = 35$ mM). The volume per injection was 7.006 μl.

interactions that may possibly underlie the mechanisms of peptide anti-microbial action.

In the case of DMPC, the broadening of the DSC curves and the decrease in T_m is compatible with a better interaction of the peptide with the liquid-crystalline phase of DMPC. As shown by other authors [22,33–35], surface insertion leads to bilayer thinning and induces an increase in local negative curvature, explaining both the lowering of T_m and the broadening of DSC curves. The observed decrease in overall ΔH as the peptide content increases, together with the referred appearance of two transitions and precipitation indicates that either the new transition has a lower energy or that part of the liposomes is no longer having a gel-to-liquid crystal transition. The decrease in ΔH indicates that the peptide is perturbing the hydrocarbon chain packing as the enthalpy for the main transition is primarily due to the disruption of intra- and intermolecular van der Waals interactions, which leads to chain melting. These results, thus, suggest that the peptide does penetrate rather deeply into the bilayer.

The appearance of shoulders in thermograms is a consequence of a non-ideal mixing behaviour,

DOI: 10.1002/psc

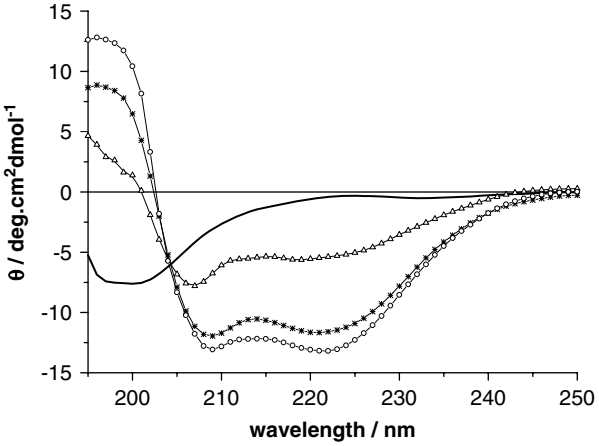

Figure 4 CD spectra ($t = 35\,^{\circ}C$) for Lyco I(1–15) 36 μM in aqueous buffer (solid line), and in the presence of LUVs of DMPC, with P : L ratio of 1 : 79 (-Δ-); DMPG, with P : L ratio of 1 : 32 (-○-) and DMPC/DMPG (3 : 1) with P : L ratio of 1 : 32 (-∗-).

which creates a non-homogeneous distribution of the peptide within the membrane. As a result, regions of two different coexisting phases, one phase richer in peptide (lower temperature) and the other lipid-rich (at the same temperature of the pure lipid or often at higher temperature) could be formed, and such domain formation has already been reported for other peptide/lipid systems [19,22,36]. Our DSC results are compatible with such events, particularly at the highest peptide ratios, where two broad transitions can be observed, each probably corresponding to a different coexisting phase. This picture, together with a highly negative enthalpy of partition to the membrane (ITC) (which is only somewhat smaller than with DMPG, after correction to the peptide that partitions to the membrane) and the clear presence of an α-helix (CD) indicates that LycoI 1–15 strongly interacts with the zwitterionic membranes, by adopting a helical secondary structure, perturbing significantly the membrane at increasing peptide content, eventually leading to membrane disruption (observed precipitation). It should be stressed that as the peptide–lipid ratio increases (at 1 : 35 and 1 : 23) the lower temperature peak is the predominant one (Table 1).

In the case of the negatively charged membrane (DMPG), a shoulder at higher temperature is also apparent at low P : L. The fact that a much more extensive precipitation was observed for this system can justify the significant decrease in enthalpy with no significant decrease in T_m – this can be interpreted as meaning that part of the liposomes are destroyed, and the remaining have a nearly unperturbed transition. Note that T_m for this high temperature peak is the same as the one for the pure lipid, within the combined uncertainties (see Table 1).

Finally, as far as the mixed system is concerned, the more close similarity to the DMPG system clearly indicates that the positively charged peptide prefers the negatively charged membrane and the presence of DMPG becomes overwhelming. Further, it is clear that the presence of 0.75% zwitterionic lipid is also not affecting the CD curve much at the low peptide ratio used (1 : 33). Therefore, at low peptide ratios, there must be a preferential partitioning to the negatively charged components of the mixed membrane.

CONCLUSIONS

The shortened analogue of LycoI, LycoI 1–15, was previously shown to have a lower leishmanicidal activity than the longer native peptide, being only active above 10 μM, but with the advantage of presenting decreased haemolytic effects [17].

The peptide adopts a α-helical structure in the presence of the three model membrane systems used.

Overall, the results showed that the peptide interacts more strongly with negatively charged lipid bilayers than with neutral membranes, energetically both (ΔH of interaction, as determined by ITC, is somewhat more exothermic for the DMPG system), in terms of partition (indirectly revealed by the difference in minima depth at 208 and 222 nm in CD curves) and in terms of the amount of precipitation/aggregation. Nevertheless, efficient perturbation of the zwitterionic DMPC systems was found, which explains the haemolytic activity. This means that more efforts have to be made towards structural optimization with the generation of peptides that will interact much less with neutral membrane systems. We believe that the low charge and the perfect amphipathicity of the LycoI 1–15 helix (all charged residues are in the same face with most hydrophobic ones on the other side) induce a good compatibility with the zwitterionic membrane, and therefore, new peptides of this family should be designed so as to at least partially disrupt this feature.

Acknowledgements

Thanks are due to FCT for financial support to Centro de Investigação em Química [CIQ(UP)], Unidade de Investigação 81. R.A. acknowledges FCT for a PhD grant (SFRH/BD/24055/2005).

REFERENCES

1. Abrunhosa F, Faria S, Gomes P, Tomaz I, Pessoa JC, Andreu D, Bastos M. Interaction and lipid-induced conformation of two cecropin-melittin hybrid peptides depend on peptide and membrane composition. *J. Phys. Chem.* 2005; **109**: 17311–17319.
2. Andreu D, Rivas L. Animal antimicrobial peptides: an overview. *Biopolymers* 1998; **47**: 415–433.

3. Appelt C, Wessolowski A, Soderhall JA, Dathe M, Schmieder P. Structure of the antimicrobial, cationic hexapeptide cyclo (RRWWRF) and its analogues in solution and bound to detergent micelles. *Chembiochem* 2005; **6**: 1654–1662.
4. Avrahami D, Shai Y. A new group of antifungal and antibacterial lipopeptides derived from non-membrane active peptides conjugated to palmitic acid. *J. Biol. Chem.* 2004; **279**: 12277–12285.
5. Benincasa M, Scocchi M, Pacor S, Tossi A, Nobili D, Basaglia G, Busetti M, Gennaro R. Fungicidal activity of five cathelicidin peptides against clinically isolated yeasts. *J. Antimicrob. Chemother.* 2006; **58**: 950–959.
6. Bhargava K, Feix JB. Membrane binding, structure and localization of Cecropin-Melittin hybrid peptides: a site-directed Spin-Labeling study. *Biophys. J.* 2004; **86**: 329–336.
7. Brogden K. Antimicrobial peptides: pore formers or metabolic inhibitors in bacteria? *Nat. Rev. Microbiol.* 2005; **3**: 238–250.
8. Chen Y, Mant CT, Farmer SW, Hancock REW, Vasil ML, GHodges RS. Rational design of a-helical antimicrobial peptides with enhanced activities and specificity/therapeutic index. *J. Biol. Chem.* 2005; **280**: 12316–12329.
9. Dathe M, Nikolenko H, Klose J, Bienert M. Cyclization increases the antimicrobial activity and selectivity of arginine- and tryptophan-containing hexapeptides. *Biochemistry* 2004; **43**: 9140–9150.
10. Ding JL, Ho B. Antimicrobial peptides: resistant-proof antibiotics of the new millennium. *Drug Dev. Res.* 2004; **62**: 317–335.
11. Esteban-Martín S, Salgado J. Self-assembling of peptide/membrane complexes by atomistic molecular dynamics simulations. *Biophys. J.* 2007; **92**: 903–912.
12. Tossi A. Host defense peptides: roles and applications. *Curr. Protein Pept. Sci.* 2005; **6**: 1–3.
13. Zasloff M. Antimicrobial peptides in health and disease. *N. Engl. J. Med.* 2002; **347**: 1199–1200.
14. Zasloff M. Antimicrobial peptides of multicellular organisms. *Nature* 2002; **415**: 389–395.
15. Lohner K, Blondelle SE. Molecular mechanisms of membrane perturbation by antimicrobial peptides and the use of biophysical studies in the design of novel peptide antibiotics. *Comb. Chem. High T. Scr.* 2005; **8**: 241–256.
16. Yan L, Adams ME. Lycotoxins, antimicrobial peptides from venom of the wolf spider Lycosa carolinensis. *J. Biol. Chem.* 1998; **273**: 2059–2066.
17. Luque-Ortega JR, Gomes P, Seixas R, Rivas L, Andreu D. Leishmanicidal activity of antimicrobial peptides from the wolf spider Lycosa carolinensis. *J. Pep. Sci.* 2006; **12**(Issue S1): 527.
18. Blume A. Applications of calorimetry to lipid model membranes. In *Physical Properties of Biological Membranes and Their Functional Implications*, Hidalgo C (ed.). Plenum Press: New York, 1988; 41–121.
19. Lohner K, Prenner EJ. Differential scanning calorimetry and X-ray diffraction studies of the specificity of the interaction of antimicrobial peptides with membrane-mimetic systems. *Biochim. Biophys. Acta* 1999; **1462**: 141–156.
20. Vogel H, Jahning F. The structure of melittin in membranes. *Biophys. J.* 1986; **50**: 573–582.
21. Wimley WC, Hristova K, Ladokhin AS, Silvestro L, Axelsen PH, White SH. Folding of b-sheet membrane proteins: a hydrophobic hexapeptide model. *J. Mol. Biol.* 1998; **277**: 1091–1110.
22. Chen HM, Leung KW, Thakur NN, Tan A, Jack RW. Distinguishing between different pathways of bilayer disruption by the related antimicrobial peptides cecropin B, B1 and B3. *Eur. J. Biochem.* 2003; **270**: 911–920.
23. Jing W, Hunter HN, Hagel J, Vogel HJ. structure of the antimicronial peptide Ac-RRWWRF-NH2 bound to micelles and its interaction with phospholipids bilayers. *J. Pept. Res.* 2003; **61**: 219–229.
24. Bishop CM, Walkenhorst WF, Wimley WC. Folding of b-sheet in membranes: specificity and promiscuity in peptide model systems. *J. Mol. Biol.* 2001; **309**: 975–988.
25. Seelig J. Thermodynamics of lipid-peptide interactions. *Biochim. Biophys. Acta* 2004; **1666**: 40–50.
26. Stella L, Mazzuca C, Venanzi M, Palleschi A, Didonè M. Aggregation and water membrane partition as major determinants of the activity of the antibiotic peptide trichogin GA IV. *Biophys. J.* 2004; **86**: 936–945.
27. White SH, Wimley WC, Ladokhin AS, Hristova K. Protein folding in membranes: determining energetics of peptide-bilayer interactions. *Meth. Enzymol.* 1998; **295**: 62–87.
28. McClare CWF. An accurate and convenient organic phosphorous assay. *Anal. Biochem.* 1971; **39**: 527–530.
29. Gomes P, Giralt E, Andreu D. Antigenicity modulation upon peptide cyclization: application of the GH loop of foot-and-mouth disease virus strain C1 – Barcelona. *Vaccine* 2001; **19**: 3459–3466.
30. Briggner L-E, Wadsö I. Test and calibration processes for microcalorimeters, with special reference to heat conduction instruments used with aqueous systems. *J. Biochem. Biophys. Methods* 1991; **22**: 101–118.
31. Matos C, Lima JL, Reis S, Lopes A, Bastos M. Interaction of antiinflammatory drugs with EPC liposomes: calorimetric study in a broad concentration range. *Biophys. J.* 2004; **86**: 946–954.
32. Bastos M, Hagg S, Lonnbro P, Wadso I. Fast titration experiments using heat conduction microcalorimeters. *J. Biochem. Biophys. Methods* 1991; **23**: 255–258.
33. Ivanova VP, Makarov IM, Schäffer TE, Heimburg T. Analyzing heat capacity profiles of peptide-containing membranes: cluster formation of Gramicidin A. *Biophys. J.* 2003; **84**: 2427–2439.
34. Ivanova VP, Heimburg T. Histogram method to obtain heat capacities in lipid monolayers, curved bilayers and membranes containing peptides. *Phys. Rev., E* 2001; **63**: 1914–1925.
35. Ladokhin AS, White SH. "Detergent-like" permeabilization of anionic lipid vesicles by melittin. *Biochim. Biophys. Acta* 2001; **1514**: 253–260.
36. Matsuzaki K, Sugishita K, Ishibe N, Ueha M, Nakata S, Miyajima K, Epand RM. Relationship of membrane curvature to the formation of pores by magainin 2. *Biochemistry* 1998; **37**: 11856–11863.